Can green roofs help with stormwater floods? A geospatial planning approach

Twohig, Cian; Casali, Ylenia; Aydin, Nazli Yonca

DOI
10.1016/j.ufug.2022.127724

Publication date
2022

Document Version
Final published version

Published in
Urban Forestry and Urban Greening

Citation (APA)
Twohig, C., Casali, Y., & Aydin, N. Y. (2022). Can green roofs help with stormwater floods? A geospatial planning approach. *Urban Forestry and Urban Greening*, *76*, Article 127724. https://doi.org/10.1016/j.ufug.2022.127724

Urban Forestry & Urban Greening 76 (2022) 127724

Contents lists available at ScienceDirect

Urban Forestry & Urban Greening

journal homepage: www.elsevier.com/locate/ufug

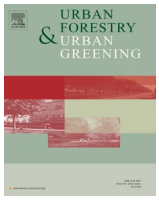

Original article

Can green roofs help with stormwater floods? A geospatial planning approach

Cian Twohig, Ylenia Casali, Nazli Yonca Aydin *

Faculty of Technology, Policy and Management, Delft University of Technology, the Netherlands

ARTICLE INFO

Handling Editor: Timothy Van Renterghem

Keywords:
Geospatial planning
Green roofs
Stormwater flooding
Resilience
Evidence-based planning

ABSTRACT

Increasing urbanization, impervious space, and the impact of climate change are threatening the future of cities. Nature-based solutions, specifically urban green infrastructures, are seen as a sustainable strategy to increase resilience against extreme weather events, including the escalating occurrence of stormwater runoff flooding. Consequently, urban planners and decision-makers have pushed their efforts toward implementing green infrastructure solutions to reduce the impact of stormwater floods. Among others, green roofs help store water and decrease stormwater runoff impacts on a local scale. This research aims to investigate the effect of surface permeability and green roof implementation on reducing stormwater flooding and subsequently provide urban planners with evidence-based geospatial planning recommendations to improve urban resilience in Helsinki. First, we modeled the current impact of stormwater flooding using the Arc-Malstrom model in Helsinki. The model was used to identify districts under high stormwater flood risk. Then, we zoomed in to a focus area and tested a combination of scenarios representing four levels of green roof implementation, two levels of green roof infiltration rates under 40-, 60-, 80-, 100 mm precipitation events on the available rooftops. We utilized open geographic data and geospatial data science principles implemented in the GIS environment to conduct this study. Our results showed that low-level implementation of green roofs with low retention rates reduces the average flood depth by only 1 %. In contrast, the maximum green roof scenario decreased most of the average flood depth (13 %) and reduced the number of vulnerable sites. The proposed methodology can be used for other cities to develop evidence-based plans for green roof implementations.

1. Introduction

Climate change impact has become more visible in cities due to the increasing intensity and duration of extreme weather events. At the same time, cities are already facing fundamental challenges related to population growth, mass urbanization, and the occurrence and expansion of urban sprawl. As a result, cities around the world, including European cities, are becoming ever-more populated and impermeable (Feng et al., 2021; D'Ambrosio et al., 2022) which makes metropolitan areas increasingly vulnerable to stormwater runoff flooding. Urban flooding consequently causes large-scale material damage to residences, infrastructures, and utility networks (Kaźmierczak and Cavan, 2011). In response to these long-term stresses and sudden shocks, resilience has been emerging and integrated into long-term strategies in national and city policies (Yumagulova and Vertinsky, 2021; Heinimann and Hatfield, 2017).

The major challenge with resilience is quantifying, measuring, and validating it. There is no methodological consensus on "how to" and "what for" to evaluate resilience in urban environments (Meerow and Newell, 2016) or for single components (e.g., water systems) (Juan-Garcia et al., 2017). Resilience is complex and multi-dimensional (e.g., Linkov and Palma-Oliveira, 2016; Bruneau and Reinhorn, 2007); it is the capacity to bouncing back from disturbances and "unexpected" events (Cutter, 2016). To this date, a systematic approach for characterizing resilience with geospatial planning is missing, in particular spatially explicit ones (Cariolet et al., 2019).

With the increasing pressure of climate change, efforts to transition towards sustainability and resilience have developed adaptation measures to integrate emerging and nature-based solutions (Lin et al., 2021). Those can lower the impact of floods, droughts, heat island effects and increase resilience against those events. However, generalizable knowledge and guidelines about the impact of complex relationships between the climate change adaptation measures and planning nature-based solutions are suffering due to the lack of comprehensive

* Corresponding author.
E-mail addresses: twohigcian@gmail.com (C. Twohig), Y.Casali@tudelft.nl (Y. Casali), N.Y.Aydin@tudelft.nl (N.Y. Aydin).

https://doi.org/10.1016/j.ufug.2022.127724
Received 27 April 2022; Received in revised form 26 July 2022; Accepted 31 August 2022
Available online 5 September 2022

investigation of costs and benefits, trade-offs, and synergies associated with these measures (Frantzeskaki et al., 2019).

Green infrastructures as nature-based solutions were promoted for systematic integration into spatial plans by European Commission in 2013 (European Commission, 2013). The benefits are, for example, increasing air quality and biodiversity, reducing heat island effects, improving stormwater management, and increasing well-being (Tran et al., 2020; Chang et al., 2021). Moreover, green infrastructures support other policies such as disaster risk management, energy transition, etc. Yet, the progress of embedding green infrastructures into spatial plans is slow because of limited understanding by stakeholders and decision-makers of green infrastructures functionality and implementation requirements, land use principles, and ecosystem services (Pozoukidou, 2020). Current struggles with green infrastructures integration also stem from the lack of evidence-based practices to outline actual economic, social and physical costs and benefits from implementations. Potentially, clear pathways and guidelines can facilitate the implementation of green infrastructure projects and increase social capital along with financial and physical capital in cities.

This research aims to create an evidence-based approach for implementing green roofs as a nature-based solution to improve urban resilience against stormwater floods. The main goal is to investigate the effect of green roof implementation on stormwater runoff in vulnerable urban districts. Therefore, this research, first, identifies the vulnerable districts to stormwater flooding; second, it measures the impact of green roof implementations under different precipitation events; and, third, it assesses the impacts of different levels of green roof implementations with varying retention rates based on proposed spatially explicit scenarios. The city of Helsinki is used as a case study to showcase our methodology. To conduct this study, we utilize open geographic data of Finland (Helsinki Region Environmental Services HSY, 2021; SYKE: Finnish Environmental Institute, 2021) and geospatial data science principles and methods. With geographic data made readily available through large open databases, evidence-based approaches can be developed to test green roof implementation strategies in Helsinki and identify geospatial factors conducive to stormwater runoff flooding (Sieker and Klein, 1998).

2. Background

As climate change is on the rise, cities are urged to take action against the increasing impacts of climate-related disasters by introducing transformation towards sustainability and resilience, both aiming to systematically understand dynamic processes and future needs in cities. More specifically, urban resilience focuses on climate adaptation and emphasizes the urgency of taking action by cities (Hoelscher and Frantzeskaki, 2021). Nature-based solutions are one of those actions that have potential to contribute to practicable climate adaptation. For example, these include green infrastructure, urban ecosystem services, and water sensitive urban design. While all of them emphasize multifunctionality and target urban challenges, the potential benefits and effectiveness of these solutions have not been discovered fully (Lin et al., 2021; Frantzeskaki and McPhearson, 2022).

The most popular and widely acknowledged urban green infrastructure solutions for sustainable stormwater drainage systems to reduce the impact of floods can be identified as green roofs, urban trees, rainwater harvesting cisterns, and the integration of permeable surfaces into pavement areas (Johnson et al., 2021). In their study, the authors conducted a scenario-based cost-benefit analysis and explored green infrastructure integration's economic and social benefits. They emphasized a tremendous economic and social value in integrating green infrastructure not only for stormwater management but also for reducing the urban heat island effect (Johnson et al., 2021). Their 3-level scenarios mainly focused on incrementally increasing green roofs and façade greening.

Similarly, Andrés-Doménech et al. (2018) investigated the performance of green roofs by comparing them with conventional roofs over a year in Valencia, Spain. Their finding also showed that even in dry climates, the green roof's contribution to hydrological processes was more significant than conventional roofs. Similar to Andrés-Doménech et al. (2018), Johnson et al. (2021) also took up three-level green roof scenarios: high green roof integration, no green roofs (i.e., baseline), and the middle range scenario where the green roof integration level would be in between the first and the second scenario.

Implementing green infrastructures in cities have rippling effects that goes beyond the location of the change. The cost and benefits of greening at one location have wider impacts in adjacent neighbourhoods. This is aligned with Tobler's first law of geography (Votsis, 2017; Tobler, 1970), which postulates that near objects are more related than distant ones. Hence, implementing of green infrastructures requires evidence-based planning and design to understand the overall impacts. Votsis (Votsis, 2017) investigated the spatial impacts of urban green infrastructure on the housing prices. Their study was based on the spatial correlation of the proximity to urban green space and city centre with the increase in the housing prices. Author found that the property values increase in close proximity to urban greening projects while the type of the green infrastructure and their proximity to the city centres would change the amount of impact on the property values. It is suggested that the urban greening projects should take into account such rippling effects to avoid igniting wider problems related to social justice e.g., increase in property values at poor neighbourhoods. On this subject, Anguelovski (Anguelovski, 2015) discussed how greening projects might become locally unwanted land uses for long-term residents in neighbourhoods as they might trigger gentrification.

While the benefits of green infrastructure implementation are clear and associated with the increase in resilience specifically in high flood risk urban areas, the effectiveness is contingent on factors such as spatial placements of green infrastructures, the conditions of urban drainage networks, and the magnitude of rainfalls (Ercolani et al., 2018). Mentens et al. (2006) investigated the impacts of green roof implementation on the stormwater runoff in Brussels, Belgium. Their results showed that converting 10 % of rooftops to green roofs could reduce the runoff by 2.7 % at the regional level and 54 % at the individual building level. Ercolani et al. (2018) hydrologically modelled green roof implementation in four different scenarios. 25 %, 50 %, 75%, and 100 % of the roof surfaces were converted to green roofs to investigate if the amount of volume reduction that green roofs provide during peak flows has a positive impact on the urban drainage network. They reported that the green roofs are more effective in terms of reduction of peak flows in small magnitude events than in larger magnitude of storms. While their study focused on the impact on urban drainage networks and hydrological processes in the urban catchment area, in our study we focus on the benefits of green roof implementation from a geospatial planning perspective in Helsinki, Finland.

Helsinki is at risk of stormwater flooding, with the use of the impervious surface area for housing, business and societal purposes resulting in low infiltration of precipitation throughout the city. The City of Helsinki has initiated the Stormwater Management Program as a further implementation of the European Union's Flood Directive (European Parlement, 2022; City of Helsinki, 2022). This program is intended to improve Helsinki's resilience to stormwater flooding and to protect the accessibility, livability, and sustainability of Helsinki in the decades to come. Moreover, Helsinki is dealing with increased urbanization and the city's population is at an all-time high (Silvennoinen et al., 2017). An influx of residents in the Finnish capital in recent decades has increased the necessity for further use of impermeable surfaces for housing (Krebs et al., 2013). To avoid turning Helsinki into a *'Concrete Jungle'*, the Urban Environment Division seeks to stabilize this increase in impermeable land surface, guaranteeing citizens sufficient living space, a high-quality living environment, and continued urban sustainability (Tiitu et al., 2020). To do so, the Urban Environment Division must strive to create permeable living environments with

sufficient capacity to house the increasing population, while bolstering the urban resilience to flooding.

Di Marino et al. (2019) reported the green infrastructure integration into spatial planning practice and policies through a literature review and identified problems and challenges in two case studies from the Helsinki-Uusimaa region and the city of Jarbenpaa, Finland. The selected case studies were analysed qualitatively based on understanding, integrating, and conflicting aspects of green infrastructure in spatial planning. The outcome of their analysis showed that narrow understanding and implementation of green infrastructure and ecosystem services is due to the fact that land use plans are quite rigid and restricted by many constraints such as land ownership and admin boundaries in Finland. In their study, they reported that city planners are asking for a concrete roadmap to regulate and plan for ecosystem services and green infrastructure. They also reported that despite the increasing efforts to promote green infrastructure and ecosystem services in Finnish national policies, administrative challenges (i.e., land ownership) and conflicting stakeholders' interests remain as main challenges to the integration of green infrastructure in land use plans. In this study, we provide a geospatial analysis by mapping the benefits of green infrastructures in Helsinki by retrofitting existing rooftops.

While some studies have looked into the potential to retrofit urban areas for integrating green infrastructure, most of them are in neighborhood-scale implementation. For example, on a neighborhood scale in Texas, USA, Thiagarajan et al. (2018) tested retrofitting green infrastructures, namely green roofs, vegetated swales, rain gardens, and permeable pavements. Their findings show annual stormwater reductions of 56 billion liters can be achieved by transitioning to green infrastructures on a single-family unit. Wiegels et al. (2021) investigated the impacts and benefits of implementing urban green infrastructures, including permeable pavements on water and energy balance at a neighborhood scale. While benefits of such transitions depend upon the level of urbanization, spatial distribution, and land cover types (i.e., site-specific). They also emphasized that the impacts and benefits of the implementation have more significant effects than the local scales. These global to local benefits should be further explored, e.g., the impact of the population density on site.

Although green roofs assist in stormwater runoff, some factors influence the efficiency and the retention rate (Speak et al., 2013). This includes local climate, relative humidity, and net radiation (Sims et al., 2016). Green roofs proved to retain more in drier climates; however, benefits remain for reducing the stormwater runoff even in dry climates (Sims et al., 2016). Another factor to consider when designing green roofs includes the structural capacity of the existing buildings. This is a critical factor when retrofitting existing rooftops as green roofs since the carrying capacity might impede building intensive green roofs with deeper soils (Castiglia Feitosa and Wilkinson, 2016). Extensive green roofs are designed with lighter vegetation, and soil layers fit better when retrofitting the existing buildings. Disadvantages exist in both green roof types. For example, intensive green roofs require more maintenance and structural modifications to implement on existing structures, while extensive green roofs might perform less when it comes to retention capacity (Castiglia Feitosa and Wilkinson, 2016).

Speak et al. (2013) conducted a case study to determine the retention capacity of intensive green roofs. They found that the median retention rate goes up to approximately 66 % in Manchester city center, UK. Furthermore, Speak et al. (2013) stated in their review of the average extensive green roof retention rate that it varies between 45 % and 60 % (Mentens et al., 2006; Stovin et al., 2012; Moran et al., 2003; DeNardo et al., 2005; VanWoert et al., 2005). Voyde et al. (2010) presented a case study to evaluate the benefits of extensive green roof implementation on stormwater runoff mitigation in Auckland, New Zealand. Authors reported that the cumulative annual retention rate of extensive green roofs is 66 %. Sims et al. (2016) conducted an experimental study to compare green roofs' retention performance under three different climatical conditions. Their results showed that the stormwater retention in drier climates could go up to 67 %, while it can reduce to 34 % in humid and maritime climates. In another pilot study, Lee et al. (2015) stated that the extensive green roofs (i.e., soil depth of 150 mm) can retain approximately 13–34 % in an urban setting located in Seoul, South Korea. Noticeably, the variability of the retention rates is considerably large in different resources. Therefore, pilot studies are necessary to determine exact retention rates, suitable types of green roofs, and efficiencies in general.

There are some studies that focus on the prioritization of green roofs in cities. Venter et al. (2021) created an interactive spatial decision support tool for prioritizing the green roof implementation in Oslo, Norway. They created a set of criteria based on the ecosystem service benefits of green roofs and involved stakeholders to explain their preferences for those criteria. High population density and spatial distribution of green spaces are used as a proxy for defining ecosystem service deficits. While their tool did not provide exact design recommendations for the implementation of green roofs, specific regions, such as the residential area in the inner city, showed higher potential for retrofitting the existing urban area and reflected more acceptance by the public. However, those studies do not explicitly state the amount of reduction of stormwater runoff that could be achieved by implementing green roofs.

Despite the lack of concrete evidence-based and spatially explicit pathways, there are also main planning principles that are agreed upon. These are connectivity, multifunctionality, and increased greening in cities, integration, multi-scale, multi-object (public, private, natural and semi-natural spaces) (Di Marino et al., 2019; Slätmo et al., 2019). While these are guiding principles, no one-size-fits-all type of solutions can be drawn for cities. Fluhrer et al. (2021) also emphasized the need for spatially explicit conditions and limitations for the implementation of urban green infrastructures, specifically in the Global South. They proposed a detailed guideline for planning multi-functional urban green infrastructure, which included design criteria for placement, dimensioning, and spatial distribution requirements for an urban area in the Global South. They mentioned that urban green infrastructures are multi-functional green spaces that serve a variety of purposes, including community building once the spatial design is done properly. Considering that currently, land is scarce in the urbanized world, finding suitable locations and defining constraints as well as opportunities for urban green infrastructure need to be adequately addressed.

Overall, in the literature, we identified that the implementation of green infrastructures, specifically green roofs, as a nature-based solution to increase urban resilience is a promising alternative. Yet, planning principles or road maps for implementing and designing green infrastructures are still missing which is haltering the wide range adaptation of nature-based solutions. In this field, there is a need to derive evidence-based knowledge to guide decision -makers, and stakeholders. Furthermore, a geospatial planning perspective needs to be comprehensively conceptualized to understand the effects of implementing green infrastructures on the reduction in stormwater runoff.

3. Material and methods

This research is composed of five main steps to test the performance of various green roof implementation options. The main framework for the methodology is given in Fig. 1.

3.1. Data collection and processing

This study was conducted in Helsinki city, the most populous city in Finland, with 648.042 residents in 2019 for 719 Km^2 (City of Helsinki, 2019). With the neighbouring cities of Espoo and Vantaa, it forms the Helsinki metropolitan area, the economic and administrative center of Finland. Helsinki is administratively divided into districts (Kaupunginosat), sub-districts (Osa-alueet), and smaller areas (Pienalueet). Here, we studied the city considering its sub-districts division because they represented the population records' smaller scale. In this work, we refer

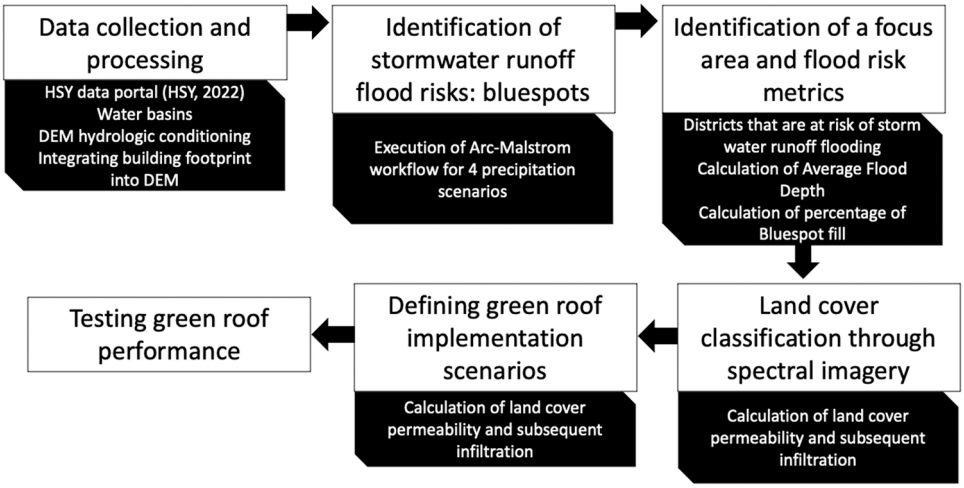

Fig. 1. Methodology of the study.

to them as neighborhoods. Open data used during this research have been acquired from several sources, primarily the Digital Elevation Model (DEM) and orthophotos provided by the National Land Survey of Finland (National Land Survey, 2021a, 2021b), the building footprint area and the green roof potential shapefiles by the Helsinki Region Environmental Services HSY (Helsinki Region Environmental Services HSY, 2021), and the neighbourhood shapefile by the Helsinki Map Service (SYKE: Finnish Environmental Institute, 2021).

The importing DEM is fundamental to producing accurate flood risk maps. In this case, the imported DEM has a resolution of 2 m and a vertical accuracy of 0.3 m, obtained through airborne laser scanning produced by the National Land Survey of Finland (National Land Survey, 2021a). The DEM is a raster dataset, consisting of a grid of cells. Each cell indicates the altitude of a 2 m^2 area in reference to sea level. Hydrologic conditioning is applied to the DEM with the object to more accurately represent the water flow direction (ESRI, 2022a). In this study, we used ArcGIS Pro (ESRI, 2022b) for all geospatial data processing steps.

The next step in procuring the required data for an initial map of Helsinki was the importation of building data, the portrayal of buildings' 'footprints' of buildings within Helsinki's borders, as well as the size, shape and area of these buildings. Data on buildings were necessary to retrieve as the stormwater runoff model could then account for the presence of impermeable structures when computing water streams, water basins and performance indicators. In order to identify the "bluespots" filled by stormwater runoff, a digital terrain model needs to be developed including both natural and man-made elevations in a raster dataset. For this, we used the toolbox Arc-Malstrom that was created by (Balstrøm and Crawford, 2018) which is integrating the building data into the digital elevation model.

3.2. Identification of stormwater runoff flood risks: bluespots

An essential component of the research is the identification of vulnerable districts in Helsinki, given different precipitation intensities. First, we need to identify areas that are under stormwater flood risk in Helsinki. A pluvial flood occurs when rainfall exceeds the capacity of the ground to store water, leading to surface runoff and overland flooding. The ground's infiltration capacity determines the amount of water that floods on the surface or permeates the soil ground. We used the Arc-Malstrom method (Balstrøm and Crawford, 2018), which implemented models to predict the stormwater flow based on Digital Terrain Model (DTM) in the ArcGIS Pro environment. A bluespot is a landscape depression where precipitation flows into and contains water. The method assumes that all precipitation falling onto a terrain within a catchment (watershed) area enters a local bluespot. When a bluespot is filled to capacity, the water flows into a neighbouring bluespot by forming a stream. The point from where it spills over is called the pour point (Balstrøm and Crawford, 2018). While bluespot model is not a complete hydrologic model, it is a very useful model when data requirements for more elaborate hydrologic models cannot be met. While it is not a continuous simulation that would include rainfall intensities, it provides a clear overview about the impacts of rainfall runoff and the amount of water that would trap in local sinks or transferred to the down streams (Balstrøm and Crawford, 2018).

We calculated the bluespots by using the DTM and building footprint areas. Taking buildings' footprint areas into account allowed for the calculation of how surface runoff divert around buildings (Balstrøm and Crawford, 2018). Besides this, the vertical accuracy of the DEM must be considered. Inaccurate input elevation data must be avoided, as it results in invalid fill up volumes of bluespot catchments. Bluespots are considered full and overflowing if the sum of the bluespot depth and vertical accuracy has reached the pour point's elevation.

After the input data are accounted for, the stormwater runoff model can be run. The model starts by rendering the DEM and filling imperfections in the raster. Following this, numerous ArcGIS Pro (ESRI, 2022b) Spatial Analyst functions are executed; as a means of computing flow directions and flow accumulation of possible water streams. Furthermore, the fill algorithm is used to determine filling depressions within the digital elevation model to identify bluespots (Planchon and Darboux, 3 2002). The output is a feature class containing the bluespots in polygon format. Next, pour points are 'snapped' to raster cell with the highest accumulation of flow, determining the spillover point of a bluespot in the process. Based on the DEM, the surrounding area's watershed is computed. Watershed is the total area contributing to filling a particular bluespot: often higher elevated ground sloping towards a depression in the surrounding area.

Once both bluespots and the watershed area are identified, nodes and edges are computed to create a network topology of flowing water streams from bluespot to bluespot. Nodes contain statistics on the volume of stormwater runoff, the capacity, and the elevation of a particular water stream. The model results in a depiction of the identified bluespots and an entire water network topology illustrating the nodes and water streams calculating spilled-over precipitation from bluespot to bluespot. Nodes and streams lying in pre-existing bodies of water are filtered out of the model manually to assure model validity.

Now that the flow direction and accumulation of stormwater runoff throughout Helsinki has been approached, we can calculate the output variables as a means of assessing the existing system's performance in deterring stormwater flooding during heavy precipitation events. This

research will calculate various output variables based on four precipitation scenarios: 40-, 60-, 80- & 100-mm precipitation events. These precipitation levels were determined based on numerous data sources predicting the occurrence of extreme precipitation events in Finland the coming century (Ruosteenoja et al., 2016).

By using the Arc-Malstrom models and accounting for 1) a drainage basin's caught stormwater volume, 2) a bluespot's spillover in volume and 3) a bluespot's spillover out volume given a level of precipitation, we were able to calculate the stormwater runoff topology (pour points and water streams), and the bluespot areas, maximum water depths and maximum fill capacities. This model does not yet account for infiltration rates.

3.3. Identification of a focus area and flood risk metrics

Once the bluespots are determined for the entire Helsinki city, we examine the size and the volume of bluespots to determine the focus area. The districts that are located in the proximity of the largest bluespot are identified as focus area to further investigate the benefits of implementing the green roof scenarios. The motivation behind selecting the largest bluespot is (1) to study if implementing green roofs will assist in reducing the impacts of floods on the neighborhoods that are more vulnerable (2) to identify how far the infiltration through land cover and implementation of different levels of green roofs with varying infiltration rates can help with the flood impact on the vulnerable locations.

Furthermore, we need to determine the flood risk metrics to be able to compare the performance of different green roof scenarios. For this purpose, we have determined two metrics to study the impact of the flood events: "average flood depth" (AFD), and the "percentage of bluespot capacity" (BF). The first metric measures the AFD throughout a neighbourhood (see Eq. 1).

$$AFD = \sum_{i=1}^{n} \frac{V_i}{(1000 * A)} \tag{1}$$

with A is the neighbourhood area and V_i is the volume of a bluespot i located within the neighbourhood. This metric was calculated for the baseline scenario, after accounting for land cover infiltration and, subsequently, for the different green roof implementation scenarios for all four of the computed precipitation events (i.e., 40-, 60-, 80- and 100-mm precipitation events).

The second metric that we evaluate is the "percentage of bluespot capacity" (BF). Bluespots can contain varying levels of stormwater. Depending on the scenario, bluespots are either empty, partially filled or full and spilling over stormwater runoff to neighbouring bluespots. Each bluespot has a watershed area, a drainage basin from which rain volume runs off into a corresponding bluespot. Having identified each bluespot's corresponding watershed area, the collected rain volume per bluespot can be computed given a certain precipitation input being collected by the watershed area. Using this computed rain volume (RV) in combination with the previously identified bluespot volume (BV) (see Eqs. 2 and 3), we were able to measure the percentage of bluespot capacity filled by stormwater (BF) (see Eq. 4).

$$RV = \quad C * \quad P/1000 \tag{2}$$

$$BV_i = RV + \quad SI_i - SO_i - I \tag{3}$$

$$BF_i = (BV_i/M_i) * 100 \tag{4}$$

RV is the volume of stormwater runoff flowing towards a designated bluespot. RV is enumerated by using the catchment area C, the surface area of the drainage basin, and the precipitation level P, the height of the precipitation caught in the drainage basin. BV_i is the stormwater volume of a bluespot i, SI_i is the spillover in and SO_i spillover out the bluespot i and I is the level of land cover infiltration. BF_i is the percentage of bluespot capacity in the bluespot i and M_i its maximum capacity. By calculating BF_i we aim to analyze the changes in the spatial distribution of bluespots capacities for all scenarios.

3.4. Land cover classification through spectral imagery

While bluespots indicate the locations where the stormwater can create a flood risk, it does not take into account the infiltration of permeability in the study area. In order to take permeability into account, we need to classify the land cover of neighbourhoods by using a spectral imagery method. The land cover determines the infiltration rate into the terrain. Therefore, we calculated the land cover to improve the flooding risk analyses.

Using multispectral imagery and a pre-determined classification dataset, land cover surfaces are classified into different categories using machine learning. This technique is commonly used to segment and classify spatial structures and surfaces throughout urban areas (Huang et al., 2007). Multi-spectral orthographic satellite images, containing three RGB-bands, are acquired from the Finnish National Land Survey (National Land Survey, 2021b). Subsequently, these 25 cm resolution JPEG2000-images are compiled using the mosaic to new raster dataset tool, providing a raster dataset ready for classification.

The classification wizard is to perform an object based, unsupervised classification of land surfaces in Helsinki given the orthographic images. This entails that the segmented groups of pixels are classified using the unsupervised ISO-cluster classifier (Nijhawan et al., 2017). The ISO-cluster classifier utilizes the K-means method to cluster pixels into land cover classes. The level of spectral detail (spectral differences between features in image) and spatial detail (the ability to distinguish different features spatially) must be established in advance. In this study, we manually identified the land cover types from the most promising spectral and spatial inputs.

The initial segmentation of the input JPEG2000 raster is dictated by the height of the input parameters. These input parameters were approached through means of trial and error. After numerous iterations of unsupervised land cover classification, the following input parameters were deemed to produce the most accurate resulting segmentation and ensuing classification of land cover. Although the majority of the input parameters retained their default values to have an optimum processing time (e.g., maximum merge distance is set to 0.5; maximum number of iterations is set to 20; merges per iteration is set to 5; skip factor is set to 10; and minimum samples per cluster is set to 20), the spectral detail, the spatial detail and the maximum number of classes were adjusted to produce a raster accurately reflecting the actuality. A higher spectral input allowed the ultimate classification to distinguish between classes of impermeable land covers, i.e., between different types of roofs, or between parking places and roads. In this study, we used the spectral detail of 15. A higher than default level of spatial detail could be afforded due to the high resolution of the input multi-spectral orthographic satellite images (25 cm). A spatial detail of 15 best reflected the spatial distinction of different land covers. Lastly, a maximum number of 10 classes was segmented, as a higher amount would lead to inaccurate segmentation causing land covers to be classified incorrectly. The above input parameters presented an accurate and comprehensive object-based classification of land cover.

After determining these input constraints, the classification wizard runs, utilizing machine learning to segment different land cover classes. Having distinguished between different land cover types, the user can manually classify which land cover type is segmented. A variety of land cover types will be used throughout this research including the classes of land cover into permeable one (grass, deciduous trees, coniferous trees and sand) and impermeable one (footpaths & roads, light grey roofs, dark grey roofs) (see Table 1).

We re-evaluated the bluespots including the impermeability effect due to the land cover classification. We approximate the average land cover infiltration per district based on land cover infiltration rates. Table 1 shows the infiltration rate per land cover used in this study with

Table 1
Land covers and the infiltration rates used in this study.

Permeability	Land Cover Class	Color in the model	Infiltration Rates	Reference
Permeable	Grass	Light Green - Yellow	20 mm/h	(Hamilton and Waddington, 1999; Regüés et al., 2017)
	Deciduous	Light Green	12 mm/h	(Butzen et al., 2015)
	Coniferous	Dark Green	8 mm/h	(Butzen et al., 2015)
	Shadow	Dark grey / black	10 mm/h	(Dare, 2005)
Impermeable	Grey Roof	Grey	0 mm/h	Assumed to be 0 mm/h due to impermeability
	Light Grey Roof	Light Grey	0 mm/h	Assumed to be 0 mm/h due to impermeability
	Asphalt	Dark Grey	0 mm/h	Assumed to be 0 mm/h due to impermeability

references. Stormwater infiltration through impermeable land covers is considered 0 mm/h. A disadvantage of land cover classification through spectral imagery is the presence of shadows due to large structures blocking the sun. These buildings are mostly surrounded by grass and impermeable surfaces; therefore, we used the average of grass and impermeable land covers to calculate the infiltrations in shadow areas. In other words, we assumed that the land cover in a given area identified as shadows, contains 50 % permeable and 50 % impermeable surfaces.

3.5. Defining green roof implementation scenarios

In this study, we analysed three classes of scenarios to evaluate the impact of runoff flooding in Helsinki; the baseline, the land cover infiltration, and the green roof scenarios. These scenarios are built considering 40-, 60-, 80- and 100-mm precipitation events. We selected the four precipitation events for all scenarios as they were previously studied in the Nordic environment (Médus et al., 2022).

Baseline scenario involves calculating the bluespots using only DEM as input data without accounting for land cover infiltration or infiltration through green roofs. In this way, we studied the bluespots and the runoff topology derived by the altitude differences and depressions in the landscape.

Land Cover Infiltration scenario investigates the effects of the land cover in the flooding. We used the infiltration rates (see Table 1) in the runoff model for this scenario. Because the land cover of neighbourhood changes, this analysis helps to study the effects of infiltration into specific neighbourhoods.

Green Roof Implementation scenarios focus on the effects of green roof implementations on flooding. Green roofs with soil depth up to 150 mm are classified as extensive green roofs (Mentens et al., 2006). Since they are light weight, and suitable for retrofitting existing rooftops (Wilkinson and Feitosa, 2015), we focus on the extensive green roof implementation on the existing rooftops in Helsinki. In this study, in order to compare the efficiency levels of green roofs, we have created two scenarios: (1) it is assumed that the retention rate from green roofs is 25 %, or (2) green roofs will provide a retention rate of 60 %. The retention rates are determined based on the literature review that we have conducted (see background section). In addition, we compared different levels of green roof implementations. Considering the available rooftops, we assumed green roofs can be implemented at the 25 %, 50 %, 75 % and 100 % of the rooftop's surfaces. We tested these scenarios for all 40-, 60-, 80- and 100-mm precipitation events. Consequently, in addition to baseline and land cover scenarios, a total of 32 scenarios were created for green roof implementations. Table 2 gives an overview of the scenarios.

4. Results and discussions

4.1. Identification of bluespots in Helsinki

Stormwater flow is modelled using the Arc-Malstrom method (Balstrøm and Crawford, 2018). The execution of the stormwater runoff flooding model provided extensive results regarding the identification of bluespots throughout Helsinki. Using the digital elevation model, terrain slope, and building data, a bluespots model was rendered. This model provides an overview of potential water catchments (and their depths) throughout the Helsinki region. For visualization purposes, bluespots with depths less than 0.05 m are not displayed in Fig. 2.A.

Bluespots are clearly prominent throughout the Helsinki region. Water catchment depths range from approximately 0.05 to 16.5 m. We found that deeper bluespots tended to occur in low altitude districts with steep slopes bordering higher elevated areas. Water catchments were found in the proximity of structural obstructions, like near road barriers, which prevented the stormwater from running off.

4.2. Identification of focus area

Bluespots are displayed with respect to their maximum water depths. We found that the largest bluespot was surrounded by Konala, Malminkartano, Marttila, Lassila, Reimarla, Kannelmaki districts (see Fig. 2. B.). Therefore, we selected them as the focus area to implement the green roof scenarios. We found that 29 % of the buildings were susceptible to floods in this area (see Fig. 2. B). Considering these buildings cover approximately 50 % of the total area in this region, it is important to investigate the impact of different range of green roof implementation with varying retention rates on the reduction of the vulnerability to stormwater floods. These districts will be further analyzed to acquire results regarding the effect of surface permeability on stormwater runoff flooding.

4.3. Land cover classification

A land cover map illustrates the different surface types given a certain area which is used to assess Helsinki's permeability. Spectral imagery and remote sensing have been utilized to classify land surface types through machine learning. After conducting the classification

Table 2
Overview of the scenarios that are considered. These scenarios are applied to 40-, 60-, 80- and 100-mm precipitation events.

Scenario	Name	Green roof implementation
Baseline	Baseline	No green roof implemented
Land cover	Land cover	No green roof implemented; infiltration rates are considered with respect to land cover classification
Green roof retention rate of 25 %	Scenario 1	Implemented on 25 % of rooftops + land cover infiltration considered
	Scenario 2	Implemented on 50 % of rooftops + land cover infiltration considered
	Scenario 3	Implemented on 75 % % of rooftops + land cover infiltration considered
	Scenario 4	Implemented on 100 % of rooftops + land cover infiltration considered
Green roof retention rate of 60 %	Scenario 5	Implemented on 25 % of rooftops + land cover infiltration considered
	Scenario 6	Implemented on 50 % of rooftops + land cover infiltration considered
	Scenario 7	Implemented on 75 % of rooftops + land cover infiltration considered
	Scenario 8	Implemented on 100 % of rooftops + land cover infiltration considered

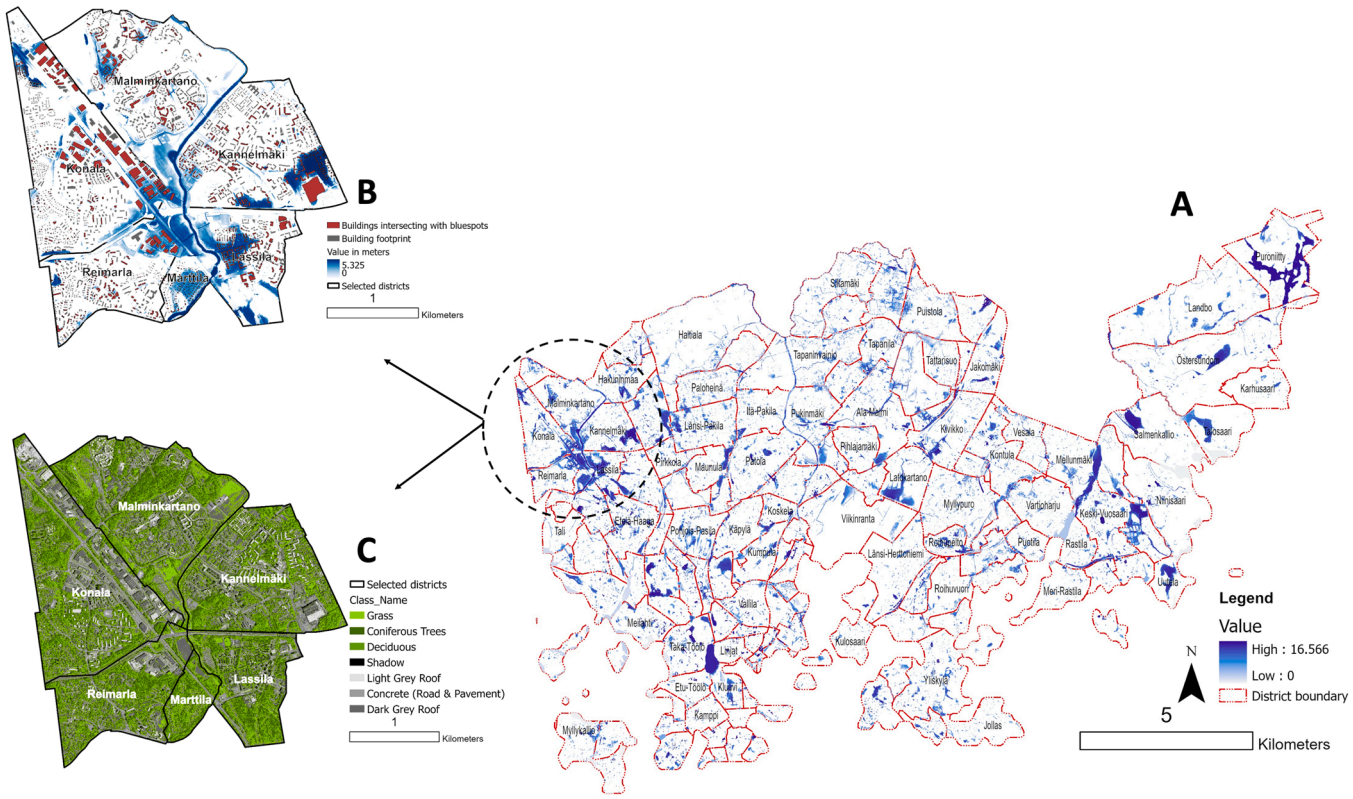

Fig. 2. A) Bluespots and corresponding depths in Helsinki. B) The bluespots and affected buildings in the study area. C) Results of the spectral imagery for land cover classification.

numerous times to assure precision and completeness, a spectral detail of 15 and a spatial detail of 15 provided the most representative object-based segmentation of pixel clusters. Fig. 2. C displays the results from the spectral imagery classification.

4.4. Assessment of flood risk metrics for proposed greenroof scenarios

4.4.1. Average flood depths

As the next step, we calculated the flood risk metrics of average flood depth (AFD) to identify if the green roof implementation and permeable land cover. Table 3 shows the changes in these metrics based on scenarios. The average flood depth decreases due to the infiltration through permeable land cover and the green roof implementation depending on the scenarios (i.e., the level of implementation and infiltration rate of the green roofs). Our results show that the incremental implementation of green roofs with a low (25 %) retention rate does not have a significant impact to reduce the average flood depth.

In Scenario 1, where we implemented green roofs on 25 % of rooftops with a retention rate of 25 % that includes land cover infiltration, the average flood depth only reduced 1 % compared to the land cover scenario for all 40-, 60-, 80- and 100-mm precipitation events. This aligns with the theory of transition and transformation (Holscher et al., 2018) that in order to reduce the impact of climate change, we need extraordinary measures and big paradigm shifts, rather than small and incremental changes. In other words, just implementing minimal measures, here represented by Scenario 1, will not show a great effect on the overall stormwater flooding reduction in the studied area. Scenario 8 decreased from 12 % to 13 % the overall AFD as compared to the Land cover scenario, which was the highest decrease that we found in scenarios 1–8. Overall, we found that the retention rates (25 % or 60 %) have a larger effect on decreasing AFD than the level of green roof implementation in scenarios 1–8. In particular, the percentual decrease in AFD more than doubled from Scenarios 1–4 to Scenarios 5–8 respectively (see Table 3). This meant that choosing the green roof setting that maximizes the green roof retention rate plays an equally important role in the planning as the extent of surface implementation.

Table 3
Percent changes in Average Flood Depth (AFD). Land cover scenario is compared with the baseline, while Scenarios 1–8 are compared with the Land cover scenario.

Scenario	Result for 40 mm		Results for 60 mm		Results for 80 mm		Results for 100 mm	
	AFD	% change	AFD	% change	AFD	% change	AFD	% change
Baseline	26	N/A	37.2	N/A	46.3	N/A	53.8	N/A
Land cover	18	-31 %	29.2	-21 %	38.3	-17 %	45.8	-15 %
Scenario 1	17.7	-1 %	28.9	-1 %	37.8	-1 %	45.2	-1 %
Scenario 2	17.5	-3 %	28.5	-3 %	37.4	-3 %	44.6	-3 %
Scenario 3	17.2	-4 %	28.1	-4%	36.9	-4 %	43.9	-4 %
Scenario 4	17	-6 %	27.7	-5 %	36.4	-5 %	43.3	-5 %
Scenario 5	17.4	-3 %	28.3	-3 %	37.2	-3 %	44.3	-3 %
Scenario 6	16.8	-7 %	27.4	-6 %	36	-6 %	42.8	-6 %
Scenario 7	16.2	-10 %	26.6	-9 %	34.8	-9 %	41.4	-10 %
Scenario 8	15.6	-13 %	25.7	-12 %	33.6	-12 %	39.9	-13 %

4.4.2. Percentage of bluespot capacity

Furthermore, we analyzed the spatial distribution of the percentage of bluespot capacity (BF) in our case study. In this study, we have baseline and land cover scenarios as well as 8 green roof scenarios for 40-, 60-, 80- and 100-mm precipitation events. We only present our results for Scenario 1 and 8 to compare the effects of implementing green roofs at minimum and maximum levels. Figs 3–6 are the results for the precipitation events of 40-, 60-, 80- and 100-mm, respectively. In these figures, the BF is presented with 4 clusters with equal intervals. The spatial comparison showed considerable differences between the baseline and the Land cover scenario at the 40 mm precipitation event. The large bluespot was full between 25 % and 50 % range in the baseline scenario while BF was reduced to 0–25 % in the Land cover scenario (see Fig. 3). The largest bluespot did not change BF clusters between scenarios for other precipitation events (see Figs. 4–6). We found that the BF level decreased at some locations. We displayed those locations with a blue circle in Figs. 3–6. Furthermore, the impacts of implementing the green roofs with 60 % retention rate at 100 % of the buildings (i.e., Scenario 8) were noticeably different at all precipitation events. These differences are marked with blue circles in Figs. 3–6. The results showed that the majority of the reduction of the BF occurred at Malminkartano district.

We found that the BF level decreased at some locations that were too small to clearly show them in the figures. Therefore, in addition to the spatial distributions, Table 4 compares the number of bluespots at each cluster for the Land cover scenario, Scenario 1 and Scenario 8. Our results show that different levels of implementation and the infiltration rates of green roofs have a considerable effect on the amount of flood reduction. For example, the number of bluespots at the 75–100 % cluster of BF was reduced by 74 % from the Land cover scenario to the Scenario 8 for the 40 mm precipitation event. As compared to Scenario 1, which decreased by 6 %, this level of decrease is considerably higher due to the high green roof retention rate and maximum level of implementation on the buildings. To reduce the number of clusters with a high value of BF (75–100 % cluster), green roofs should be implemented with the highest infiltration rates at all buildings (i.e., Scenario 8). Whereas, we found that the number of clusters with low values of BF (0–0.25 % and 0.25–0.50 % clusters) increased for Scenario 8. The reason is that clusters with high-values BF became clusters with less volume of flooded water. This result showed that Scenario 8 helps to reduce the exposure to the high-volume flooded locations and therefore decrease flood vulnerabilities linked with high-volume flooded locations.

The implementation of green roofs helped the most when the precipitation event was low (i.e., 40 mm). The number of bluespots at the 75–100 % cluster was reduced at Scenario 8 by 74 % at 40-mm precipitation event, while it was reduced by 52–57 % for the other precipitation events (see Table 4). This finding is in line with the (Ercolani et al., 2018) who reported the effectiveness level of the green roofs in small magnitude of precipitation.

5. Conclusion and future work

The aim of this research was to investigate the effect of green roof implementations on stormwater runoff flooding in Helsinki's vulnerable districts, as a means of providing evidence-based approach for improving Helsinki's urban resilience to flooding. The ensuing results form the foundation for the establishment of sensible urban land-use policies by the City of Helsinki Urban Environment Division, allowing for the sustainable growth of Helsinki's population and urban area. The research commenced by investigating Helsinki's districts with the highest flood risk in 40-, 60-, 80- and 100-mm precipitation scenarios. Malminkartano, Kannelmaki, Konala, Lassila, Marttila, and Reimarla were identified as Helsinki's districts most vulnerable to stormwater runoff flooding.

The utilized model for bluespot identification (Balstrøm and Crawford, 2018) clearly illustrated that relatively low-lying districts are at

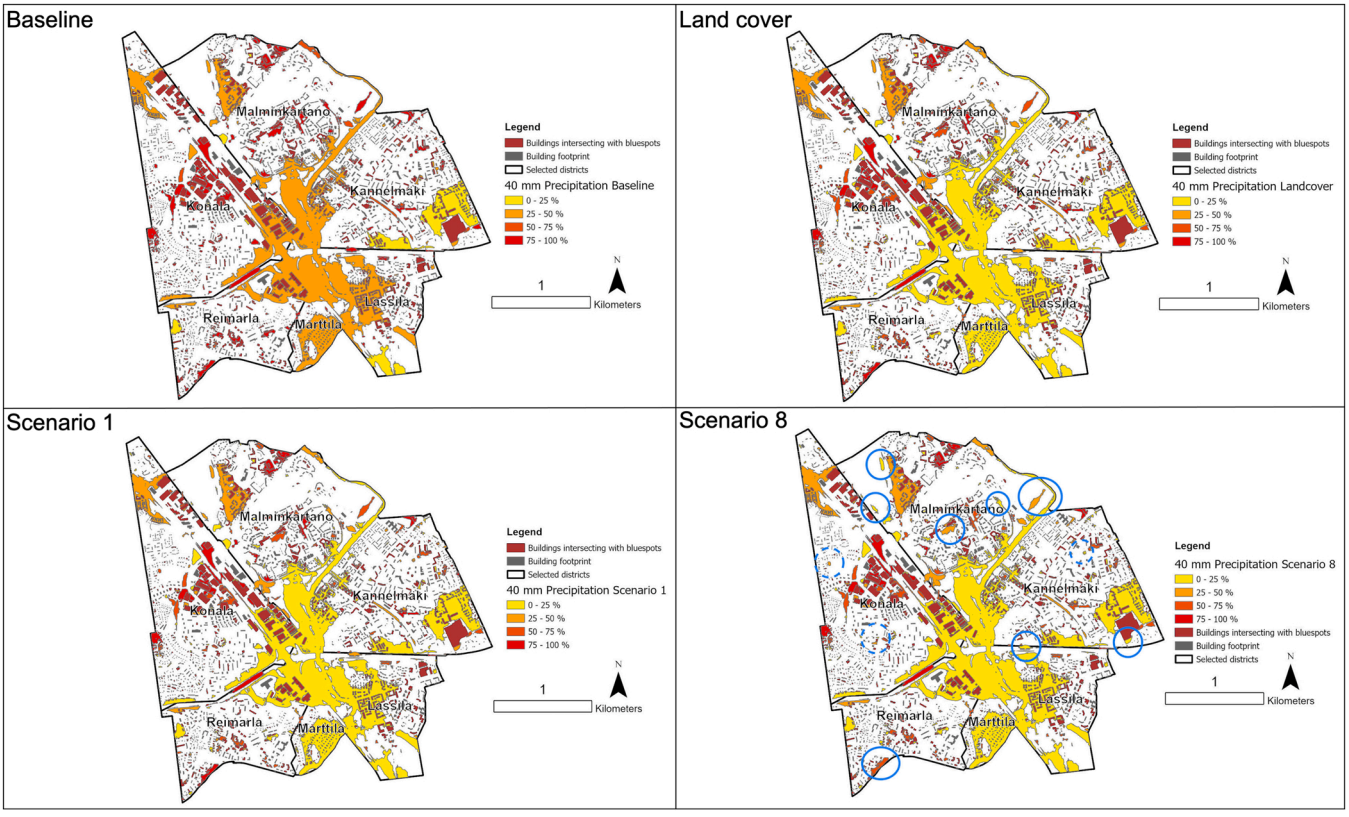

Fig. 3. 40 mm precipitation event. Blue circles mark the major differences between the Scenarios 1 and 8, dashed circles mark some of the minor differences between the Scenarios 1 and 8.

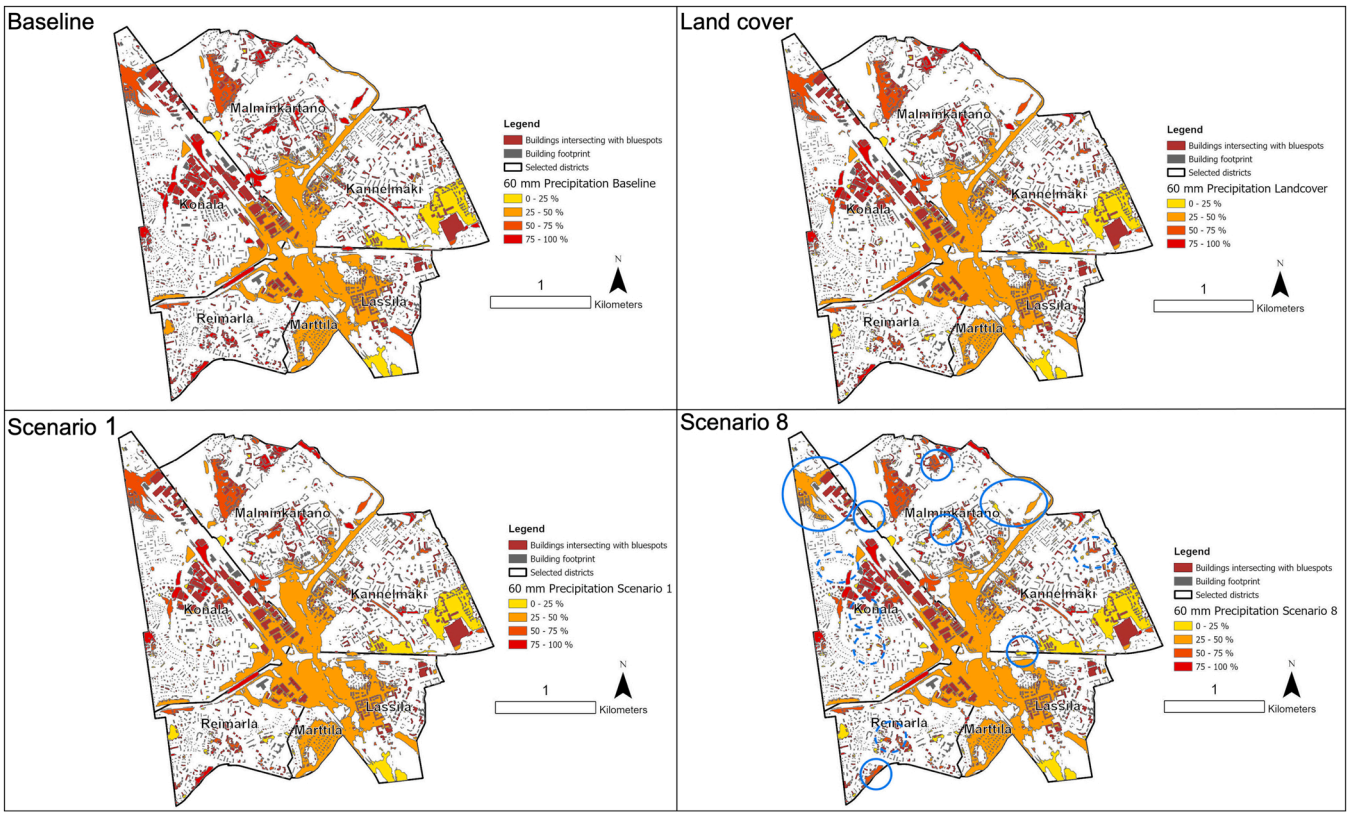

Fig. 4. 60 mm precipitation event. Blue circles mark the major differences between the Scenarios 1 and 8, dashed circles mark some of the minor differences between the Scenarios 1 and 8.

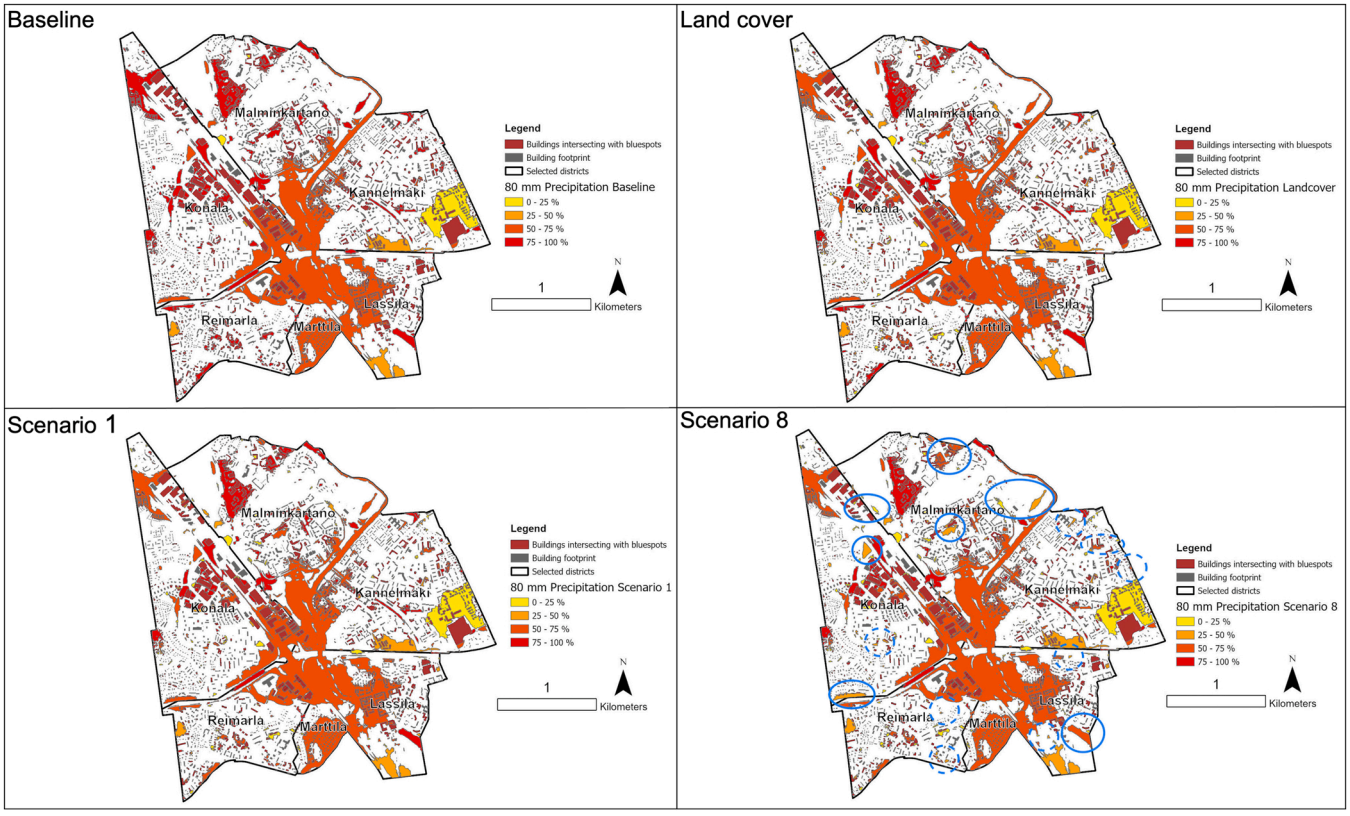

Fig. 5. 80 mm precipitation event. Blue circles mark the major differences between the Scenarios 1 and 8, dashed circles mark some of the minor differences between the Scenarios 1 and 8.

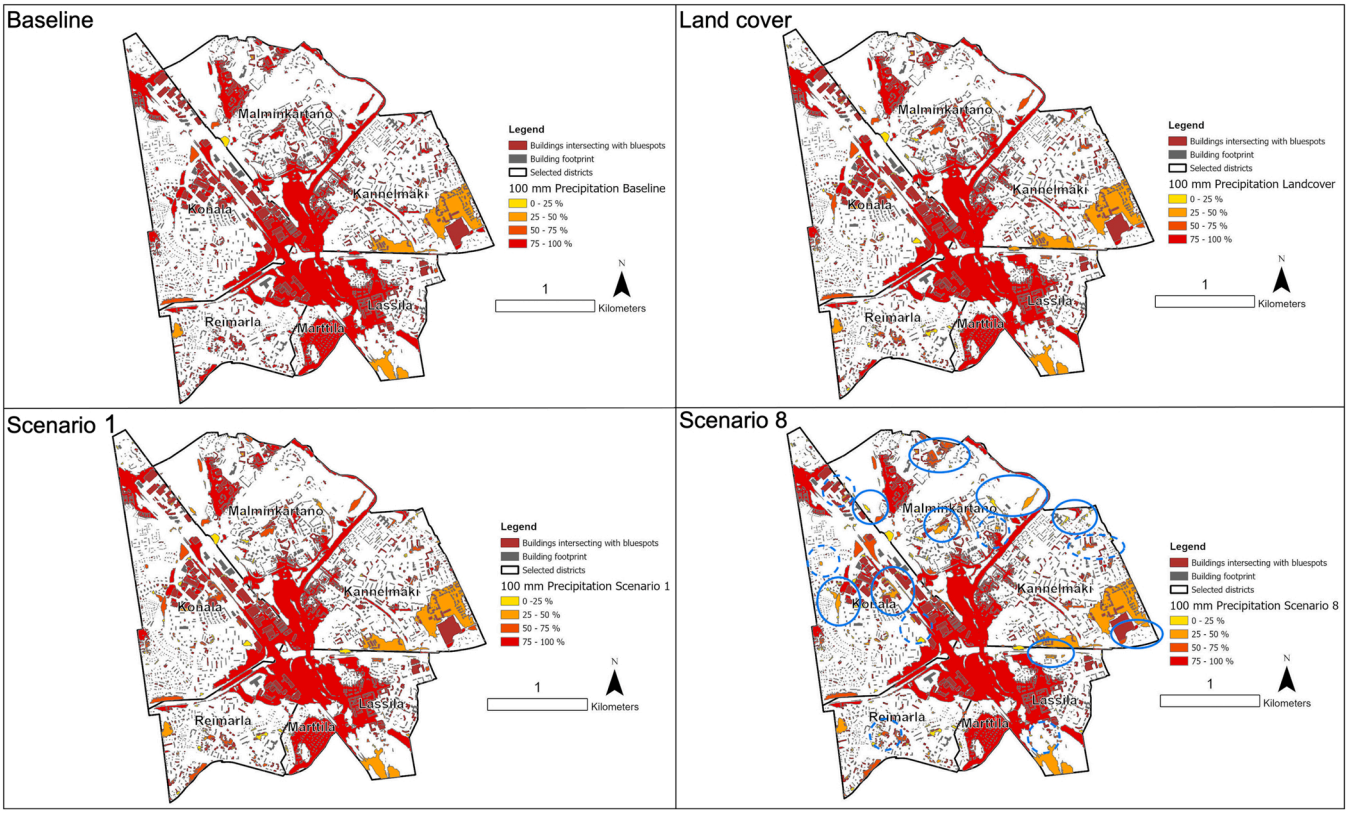

Fig. 6. 100 mm precipitation event. Blue circles mark the major differences between the Scenarios 1 and 8, dashed circles mark some of the minor differences between the Scenarios 1 and 8.

Table 4
Number of bluespots at each cluster reported for each scenario. We calculated the percent changes by comparing the number of bluespots in Scenario 1 and 8 with the Land cover scenario.

Precipitation	Scenarios	Number of bluespots at each cluster Total # of bluespots in the study area is 696							
		0–25 %	% change	25–50%	% change	50–75%	% change	75–100%	% change
40 mm	Land cover	221		146		233		96	
	Scenario 1	228	3 %	145	-1 %	233	0 %	90	-6 %
	Scenario 8	279	26 %	147	1 %	245	5 %	**25**	**-74 %**
60 mm	Land cover	204		115		202		175	
	Scenario 1	212	4 %	112	-3 %	209	3 %	163	-7 %
	Scenario 8	280	37 %	127	10 %	212	5 %	**77**	**-56 %**
80 mm	Land cover	196		100		193		207	
	Scenario 1	210	7 %	93	-7 %	204	6 %	189	-9 %
	Scenario 8	286	46 %	121	21 %	189	-2 %	**100**	**-52 %**
100 mm	Land cover	194		95		180		227	
	Scenario 1	210	8 %	88	-7 %	189	5 %	209	-8 %
	Scenario 8	304	57 %	119	25 %	176	-2 %	**97**	**-57 %**

risk of stormwater runoff flooding, as precipitation descends from higher-elevated water catchments. Subsequently, to determine the effect of land-use composition on the permeable to impermeable surface ratio in these districts, the land cover types of these districts were classified. Results were garnered indicating that increased permeability via green roof implementation positively affects a district's ability to infiltrate stormwater.

Furthermore, we investigated the effects of green roof implementation with different infiltration rates and level of applications. However, exclusively infiltration through green roof implementation with low infiltration rate (i.e., 25 %) on a quarter of buildings proved to be too little (i.e., 1 %, see Table 3) for reducing the average flood depth. Therefore, Scenario 1 did not comprehensively contribute to urban resilience in the selected districts. Instead, we found that implementing green roofs with a high infiltration rate (i.e., 60 %) on all available buildings (i.e., Scenario 8) could potentially reduce the average flood depth and the percentage of bluespot capacities. However, it should be noted that future geospatial plans should focus on increasing permeable surfaces together with the green roof options to be able to ensure the resilience in Helsinki. A general recommendation for all urban environments at risk of stormwater runoff flooding is to proactively identify potential water catchments based on geological characteristics. Following this, a hydrological assessment can be conducted to specify if water catchments are likely to overflow during extreme precipitation events. The permeability of these water catchments can subsequently be prioritized in land-use policies, as infiltration reduces stormwater concentrated in water catchments.

This research contributed to a broader audience in the field of urban

green roof and nature-based solutions. First, this work introduced a reproducible methodology that quantitatively detects changes in green roof implementations by using open urban geospatial data. The modeling approach of this research measure the impact of flooding and green roof retention by using geospatial features at a local scale. Therefore, it extends the modeling approach of (Wiegels et al., 2021), who used a grid-based model to evaluate the impact of urban green infrastructures on water and energy balance. Moreover, our approach helps visually identifying the changing impact of flooding on maps (see Figs. 3–6), which extends the analytical approach of (Speak et al., 2013; Castiglia Feitosa and Wilkinson, 2016), who did not demonstrate any geospatial distribution of green roof impacts in their assessments.

Second, this work shows how open geospatial data and analysis can contribute to developing urban solutions against common natural threats, such as stormwater flooding events. The research strives to provide urban planners and policymakers with sufficient results to establish evidence-based yet sensible land-use policies. The results from the proposed method can help policymakers detecting neighborhoods that need more resources and adapting their policies by considering at different scenarios. Consequently, urban planners could use the outcomes of our research as an evidence-based decision support tool to compare different green roof implementation scenarios at the neighborhood scale and take informed actions for future urban plans. While the proposed methodology is demonstrated in a case study from Helsinki city, the approach presented here could easily be applied to any other city worldwide where required data is available. Using this methodology in more case studies would help to achieve generalizable guidelines and frameworks to implement green roofs in cities.

Future research can focus on enhancing the applied methodology, for instance by utilizing continuous simulation to investigate flood risk during extreme precipitation events in real-time. This can facilitate the simulation of a potential stormwater runoff drainage system. Moreover, the relationship between permeability, population density, and population dense residential areas consisting of large, impermeable apartment complexes must be further examined and verified in future research. Lastly, a cost-benefit analysis of the suggested interventions can be conducted for practical implementation on local-scale in Helsinki. Should these steps be carried out, then Helsinki's urban resilience to floods will inevitably be improved, leading to an accessible, livable, sustainable, and hopefully permeable future for generations to come.

Throughout the process of researching Helsinki's urban resilience to flooding, varying research limitations at times curtailed the investigation of this research. First, the Arc-Malstrom model (Balstrøm and Crawford, 2018) is a 1D hydrologic model to assess the stormwater impacts. Currently, stormwater modelling using the Arc-Malstrom model and GIS cannot be seen as continuous simulation. Therefore, variables such as rainfall intensity (mm/hour) and infiltration rate (mm/hour) could not be simulated over continuous time intervals. During this research, the executed model represented precipitation events, where a fixed amount of rain volume precipitated into water catchments and potentially flowed downhill in accordance with Horton flow mechanisms. However, as stated, real-time continuous simulation is not facilitated by GIS. To further verify the results of this research, one could consider implementing a continuous simulation of the research scope to investigate the impact of rainfall intensities along within the context of green roof implementation strategies. Unfortunately, due to this constraint hydrological processes, such as the draining of stormwater runoff through drainage systems, could not be added to the model. Although continuous hydrological simulation carries a computational burden, it may be worthwhile to include this in future research to provide a more realistic and precise simulation of the urban stormwater cycle.

Secondly, due to limitations in the adaptation of the stormwater runoff model, the effect of permeability on the variables such as percentage of flooded area and number of affected buildings could not be investigated spatially explicitly. Although average flood depth and percentage of the bluespot capacities provided an indication of the effect of permeability on flooding vulnerability in Helsinki's districts, discrepancies between e.g., average flood depth and the percentage of flooded area would have been interesting and may have provided a more in-depth view of the effect of permeability on urban resilience to flooding. This detail should be kept in mind when interpreting the results and considering future research. Furthermore, the land cover classification accuracy was done by trial and error using GIS and only tested visually by comparing JPEG images with the classification results due to the lack of ground truth (i.e., field) data. Future studies should investigate the accuracy by comparing ground truth and classification results using, for example, kappa index. Finally, due to computational resources and time constraints, the permeability of only five vulnerable districts in Helsinki was investigated extensively. Although these districts clearly gave an initial indication of the effect of permeability on stormwater runoff flooding, future research may consider a larger sample size to acquire more results that can be generalized easier.

CRediT authorship contribution statement

Cian Twohig: Conceptualization, Software, Validation, Formal analysis, Investigation, Data curation Writing – review & editing, Ylenia Casali: Conceptualization, Methodology, Resources, Writing – original draft, Writing – review & editing, Supervision, Nazli Yonca Aydin: Conceptualization, Methodology, Validation, Investigation, Resources, Writing – original draft, Writing – review & editing, Visualization, Supervision, Project administration.

Declaration of Competing Interest

The authors declare that they have no known competing financial interests or personal relationships that could have appeared to influence the work reported in this paper.

Data availability

To conduct this study, we utilize open geographic data of Finland. https://kartta.hsy.fi/ https://www.syke.fi/en.

References

Andrés-Doménech, I., Perales-Momparler, S., Morales-Torres, A., Escuder-Bueno, I., 2018. Hydrological performance of green roofs at building and city scales under mediterranean conditions. Sustainability 10 (9). https://doi.org/10.3390/su10093105.

Anguelovski, I., 2015. From toxic sites to parks as (Green) LULUs? New challenges of inequity, privilege, gentrification, and exclusion for urban environmental justice. J. Plan. Lit. 31 (1), 23–36. https://doi.org/10.1177/0885412215610491.

Balstrøm, T., Crawford, D., 2018. Arc-Malstrøm: a 1D hydrologic screening method for stormwater assessments based on geometric networks. Comput. Geosci. 116, 64–73. https://doi.org/10.1016/j.cageo.2018.04.010.

Bruneau, M., Reinhorn, A., 2007. Exploring the concept of seismic resilience for acute care facilities. Earthq. Spectra 23 (1), 41–62. https://doi.org/10.1193/1.2431396.

Butzen, V., et al., 2015. Water repellency under coniferous and deciduous forest — experimental assessment and impact on overland flow. Catena 133, 255–265. https://doi.org/10.1016/j.catena.2015.05.022.

Cariolet, J.-M., Vuillet, M., Diab, Y., 2019. Mapping urban resilience to disasters – a review. Sustain. Cities Soc. 51 https://doi.org/10.1016/j.scs.2019.101746.

Castiglia Feitosa, R., Wilkinson, S., 2016. Modelling green roof stormwater response for different soil depths. Landsc. Urban Plan. 153, 170–179. https://doi.org/10.1016/j.landurbplan.2016.05.007.

Chang, H.-S., Lin, Z.-H., Hsu, Y.-Y., 2021. Planning for green infrastructure and mapping synergies and trade-offs: a case study in the Yanshuei River Basin, Taiwan. Urban For. Urban Green. 65 https://doi.org/10.1016/j.ufug.2021.127325.

City of Helsinki. "2019 Statistical Yearbook of Helsinki." ⟨https://www.hel.fi/hel2/tietokeskus/julkaisut/pdf/20_03_10_Vuosikirjaenglanti2019.pdf⟩ (accessed 25 March, 2022).

City of Helsinki. "City of Helsinki Storm Water Management Program." ⟨https://www.hel.fi/static/liitteet/kaupunkiymparisto/julkaisut/julkaisut/julkaisu-03–18-en.pdf⟩. (accessed 25 March, 2022).

Cutter, S.L., 2016. Resilience to what? Resilience for whom? Geogr. J. 182 (2), 110–113. https://doi.org/10.1111/geoj.12174.

D'Ambrosio, R., Balbo, A., Longobardi, A., Rizzo, A., 2022. Re-think urban drainage following a SuDS retrofitting approach against urban flooding: a modelling investigation for an Italian case study. Urban For. Urban Green. 70 https://doi.org/10.1016/j.ufug.2022.127518.

Dare, P.M., 2005. Shadow analysis in high-resolution satellite imagery of urban areas. Photogramm. Eng. Remote Sens. 71 (2), 169–177. https://doi.org/10.14358/Pers.71.2.169.

DeNardo, J., Jarrett, A., Manbeck, H., Beattie, D., Berghage, R., 2005. Stormwater mitigation and surface temperature reduction by green roofs. Trans. ASAE vol. 48 (4), 1491–1496.

Di Marino, M., Tiitu, M., Lapintie, K., Viinikka, A., Kopperoinen, L., 2019. Integrating green infrastructure and ecosystem services in land use planning. Results from two Finnish case studies. Land Use Policy 82, 643–656. https://doi.org/10.1016/j.landusepol.2019.01.007.

Ercolani, G., Chiaradia, E.A., Gandolfi, C., Castelli, F., Masseroni, D., 2018. Evaluating performances of green roofs for stormwater runoff mitigation in a high flood risk urban catchment. J. Hydrol. 566, 830–845. https://doi.org/10.1016/j.jhydrol.2018.09.050.

ESRI. "ArcGIS Pro." ⟨https://www.esri.com/en-us/arcgis/products/arcgis-pro/overview⟩ (accessed 25 March, 2022b).

ESRI. "Creating a hyrologically conditioned DEM." ⟨https://proceedings.esri.com/library/userconf/proc15/tech-workshops/tw_897–156.pdf⟩ (accessed 25 March, 2022a).

European Commission, "Green Infrastructure (GI) — Enhancing Europe's Natural Capital," 2013. [Online]. Available: ⟨https://eur-lex.europa.eu/resource.html?uri=cellar:d41348f2–01d5–4abe-b817–4c73e6f1b2df.0014.03/DOC_1&format=PDF⟩.

European Parlement. "DIRECTIVE 2007/60/EC: On the assessment and management of flood risks." ⟨https://eur-lex.europa.eu/legal-content/EN/TXT/HTML/?uri=CELEX:32007L0060&from=EN⟩. (accessed 25 March, 2022).

Feng, B., Zhang, Y., Bourke, R., 2021. Urbanization impacts on flood risks based on urban growth data and coupled flood models. Nat. Hazards 106 (1), 613–627. https://doi.org/10.1007/s11069-020-04480-0.

Fluhrer, T., Chapa, F., Hack, J., 2021. A Methodology for assessing the implementation potential for retrofitted and multifunctional urban green infrastructure in public areas of the Global South. Sustainability vol. 13 (1). https://doi.org/10.3390/su13010384.

Frantzeskaki, N., et al., 2019. Nature-based solutions for urban climate change adaptation: linking science, policy, and practice communities for evidence-based decision-making. BioScience 69 (6), 455–466. https://doi.org/10.1093/biosci/biz042.

Frantzeskaki, N., McPhearson, T., 2022. Mainstream nature-based solutions for urban climate resilience. Bioscience 72 (2), 113–115. https://doi.org/10.1093/biosci/biab105.

Hamilton, G.W., Waddington, D.V., 1999. Infiltration rates on residential lawns in central Pennsylvania. J. Soil Water Conserv. 54 (3), 564–568. ⟨https://www.jswconline.org/content/jswc/54/3/564.full.pdf⟩.

Heinimann, H.R., Hatfield, K., 2017. Infrastructure resilience assessment, management and governance – state and perspectives. Dordrecht. Springer Netherlands, in Resilience and Risk,, pp. 147–187.

Helsinki Region Environmental Services HSY. "HSY: Open Data." ⟨https://kartta.hsy.fi/⟩ (accessed 12 May, 2021).

Hoelscher, K., Frantzeskaki, N., 2021. Perspectives on urban transformation research: transformations in, of, and by cities. Urban Transform. 3 (2) https://doi.org/10.1186/s42854-021-00019-z.

Hölscher, K., Wittmayer, J.M., Loorbach, D., 2018. Transition versus transformation: what's the difference? Environ. Innov. Soc. Transit. 1–3. https://doi.org/10.1016/j.eist.2017.10.007.

Huang, X., Zhang, L., Li, P., 2007. Classification and extraction of spatial features in urban areas using high-resolution multispectral imagery. IEEE Geosci. Remote Sens. Lett. 4 (2), 260–264. https://doi.org/10.1109/lgrs.2006.890540.

Johnson, D., Exl, J., Geisendorf, S., 2021. The potential of stormwater management in addressing the urban heat island effect: an economic valuation. Sustainability vol. 13 (16). https://doi.org/10.3390/su13168685.

Juan-Garcia, P., et al., 15 2017. Resilience theory incorporated into urban wastewater systems management. State of the art. Water Res. 115, 149–161. https://doi.org/10.1016/j.watres.2017.02.047.

Kaźmierczak, A., Cavan, G., 2011. Surface water flooding risk to urban communities: analysis of vulnerability, hazard and exposure. Landsc. Urban Plan. 103 (2), 185–197. https://doi.org/10.1016/j.landurbplan.2011.07.008.

Krebs, G., Rimpiläinen, U.-M., Salminen, O., 2013. How does imperviousness develop and affect runoff generation in an urbanizing watershed? Fenn. – Int. J. Geogr. 143–159. https://doi.org/10.11143/7794.

Lee, J.Y., Lee, M.J., Han, M., 2015. A pilot study to evaluate runoff quantity from green roofs. J. Environ. Manag. 152, 171–176. https://doi.org/10.1016/j.jenvman.2015.01.028.

Lin, B.B., et al., 2021. Integrating solutions to adapt cities for climate change. Lancet Planet. Health 5 (7), e479–e486. https://doi.org/10.1016/s2542-5196(21)00135-2.

Linkov, I., Palma-Oliveira, J.M., 2016. Resilience and Risk Methods and Application in Environment, Cyber and Social Domains. Proceedings of the NATO Advanced Research Workshop on Resilience-Based Approaches to Critical Infrastructure.

Médus, E., et al., 2022. Characteristics of precipitation extremes over the Nordic region: added value of convection-permitting modeling. Nat. Hazards Earth Syst. Sci. vol. 22 (3), 693–711. https://doi.org/10.5194/nhess-22-693-2022.

Meerow, S., Newell, J.P., 2016. Urban resilience for whom, what, when, where, and why? Urban Geogr. 40 (3), 309–329. https://doi.org/10.1080/02723638.2016.1206395.

Mentens, J., Raes, D., Hermy, M., 2006. Green roofs as a tool for solving the rainwater runoff problem in the urbanized 21st century? Landsc. Urban Plan. 77 (3), 217–226. https://doi.org/10.1016/j.landurbplan.2005.02.010.

Moran, A., Hunt, B., Jennings, G., 2003. A North Carolina field study to evaluate greenroof runoff quantity, Runoff Quality, and Plant Growth. World Water Environ. Resour. Congr. 2003, 1–10.

National Land Survey. " National Land Survey of Finland: Digital Elevation Model." ⟨https://tiedostopalvelu.maanmittauslaitos.fi/tp/kartta?lang=en⟩ (accessed 1 January, 2021a).

National Land Survey. "National Land Survey of Finland: Orthophotos." ⟨https://www.maanmittauslaitos.fi/en/maps-and-spatial-data/expert-users/product-descriptions/orthophotos⟩ (accessed 1 January, 2021b).

Nijhawan, R., Srivastava, I., Shukla, P., 2017. Land cover classification using supervised and unsupervised learning techniques. 2017 Int. Conf. Comput. Intell. Data Sci. (Iccids). https://doi.org/10.1109/iccids.2017.8272630.

Planchon, O., Darboux, F., 2002. A fast, simple and versatile algorithm to fill the depressions of digital elevation models. Catena 46 (2–3), 159–176. https://doi.org/10.1016/S0341-8162(01)00164-3.

Pozoukidou, G., 2020. Designing a green infrastructure network for metropolitan areas: a spatial planning approach. Eur. -Mediterr. J. Environ. Integr. 5 (2) https://doi.org/10.1007/s41207-020-00178-8.

Regüés, D., et al., 2017. Analysing the effect of land use and vegetation cover on soil infiltration in three contrasting environments in northeast Spain. Cuad. De. Invest. Geográfica 43 (1). https://doi.org/10.18172/cig.3164.

Ruosteenoja, K., Jylhä, K., Kämäräinen, M., 2016. Climate projections for Finland under the RCP forcing scenarios. Geophysica 51 (1), 17–50.

Sieker, H., Klein, M., 1998. Best Management Practices for stormwater-runoff with alternative methods in a large urban catchment in Berlin, Germany. Water Sci. Technol. 38 (10), 91–97. https://doi.org/10.1016/S0273-1223(98)00737-9.

Silvennoinen, S., Taka, M., Yli-Pelkonen, V., Koivusalo, H., Ollikainen, M., Setälä, H., 2017. Monetary value of urban green space as an ecosystem service provider: a case study of urban runoff management in Finland. Ecosyst. Serv. 28, 17–27. https://doi.org/10.1016/j.ecoser.2017.09.013.

Sims, A.W., et al., 2016. Retention performance of green roofs in three different climate regions. J. Hydrol. 542, 115–124. https://doi.org/10.1016/j.jhydrol.2016.08.055.

Slätmo, E., Nilsson, K., Turunen, E., 2019. Implementing green infrastructure in spatial planning in Europe. Land 8 (4). https://doi.org/10.3390/land8040062.

Speak, A.F., Rothwell, J.J., Lindley, S.J., Smith, C.L., 2013. Rainwater runoff retention on an aged intensive green roof. Sci. Total Environ. 461–462, 28–38. https://doi.org/10.1016/j.scitotenv.2013.04.085.

Stovin, V., Vesuviano, G., Kasmin, H., 2012. The hydrological performance of a green roof test bed under UK climatic conditions. J. Hydrol. 414–415, 148–161. https://doi.org/10.1016/j.jhydrol.2011.10.022.

SYKE: Finnish Environmental Institute. "Downloadable spatial datasets - syke.fi." ⟨https://www.syke.fi/en⟩ (accessed 2021, 20 April).

Thiagarajan, M., Newman, G., Van Zandt, S., 2018. The projected impact of a neighborhood-scaled green infrastructure retrofit. Sustainability 10 (10). https://doi.org/10.3390/su10103665.

Tiitu, M., Naess, P., Ristimäki, M., 2020. The urban density in two Nordic capitals – comparing the development of Oslo and Helsinki metropolitan regions. Eur. Plan. Stud. 29 (6), 1092–1112. https://doi.org/10.1080/09654313.2020.1817865.

Tobler, W.R., 1970. A computer movie simulating urban growth in the Detroit Region. Econ. Geogr. 46, 234–240. https://doi.org/10.2307/143141.

Tran, T.J., Helmus, M.R., Behm, J.E., 2020. Green infrastructure space and traits (GIST) model: Integrating green infrastructure spatial placement and plant traits to maximize multifunctionality. Urban For. Urban Green. 49 https://doi.org/10.1016/j.ufug.2020.126635.

VanWoert, N.D., Rowe, D.B., Andresen, J.A., Rugh, C.L., Xiao, L., 2005. Watering regime and green roof substrate design affect Sedum plant growth. HortScience 40 (3), 659–664.

Venter, Z.S., Barton, D.N., Martinez-Izquierdo, L., Langemeyer, J., Baró, F., McPhearson, T., 2021. Interactive spatial planning of urban green infrastructure – Retrofitting green roofs where ecosystem services are most needed in Oslo. Ecosyst. Serv. 50 https://doi.org/10.1016/j.ecoser.2021.101314.

Votsis, A., 2017. Planning for green infrastructure: the spatial effects of parks, forests, and fields on Helsinki's apartment prices. Ecol. Econ. 132, 279–289. https://doi.org/10.1016/j.ecolecon.2016.09.029.

Voyde, E., Fassman, E., Simcock, R., 2010. Hydrology of an extensive living roof under sub-tropical climate conditions in Auckland, New Zealand. J. Hydrol. 394 (3–4), 384–395. https://doi.org/10.1016/j.jhydrol.2010.09.013.

Wiegels, R., Chapa, F., Hack, J., 2021. High resolution modeling of the impact of urbanization and green infrastructure on the water and energy balance. Urban Clim. 39 https://doi.org/10.1016/j.uclim.2021.100961.

Wilkinson, S., Feitosa, R., 2015. Retrofitting housing with lightweight green roof technology in Sydney, Australia, and Rio de Janeiro, Brazil. Sustainability 7 (1), 1081–1098. https://doi.org/10.3390/su7011081.

Yumagulova, L., Vertinsky, I., 2021. Managing trade-offs between specific and general resilience: insights from Canada's Metro Vancouver region. Cities 119. https://doi.org/10.1016/j.cities.2021.103319.